Effective Radius of Cloud Droplets by Ground-Based Remote Sensing: Relationships to Aerosol?

B.-G. Kim, S. E. Schwartz, and M. A. Miller
Environmental Sciences Department
Brookhaven National Laboratory
Upton, New York

Q.-L. Min
Atmospheric Science Research Center
State University of New York
Albany, New York

Introduction

Aerosol Indirect Effect

Increases in anthropogenic sources of cloud condensation nuclei can increase cloud albedo by increasing the concentration and reducing the size of cloud droplets, usually referred to as the indirect effect of aerosol on climate (Twomey 1977). However, the magnitudes of the various kinds of indirect forcing are particularly uncertain, because they involve subtle changes in cloud radiative properties and lifetimes (Schwartz and Slingo 1996).

Why Ground-Based Remote Sensing?

Studies relating the enhancement of cloud droplet concentrations to the increase of cloud albedo have typically limited to in-situ and remotely sensed characterization of cloud microphysics during the intensive field campaigns, such as International Climatology Program (Radke et al. 1989), Atlantic Stratocummulus Transition Experiment (ASTEX) (Albrecht et al. 1995), and Aerosol Characterization Experiment-2 (ACE-2) (Brenguier et al. 2000).

The U.S. Department of Energy's (DOE's) Atmospheric Radiation Measurement (ARM) Program established the Southern Great Plains (SGP) and North Slope of Alaska (NSA) Cloud and Radiation Testbed (CART) sites to conduct multiple continuous in situ and remote measurements of radiation and cloud and aerosol properties over the extended periods (Stokes and Schwartz 1994). Surface remote sensing has the advantage of continuous operation over long periods and can examine long-term trends in aerosol properties (Figure 1). Key measurements and instruments are shown in Table 1.

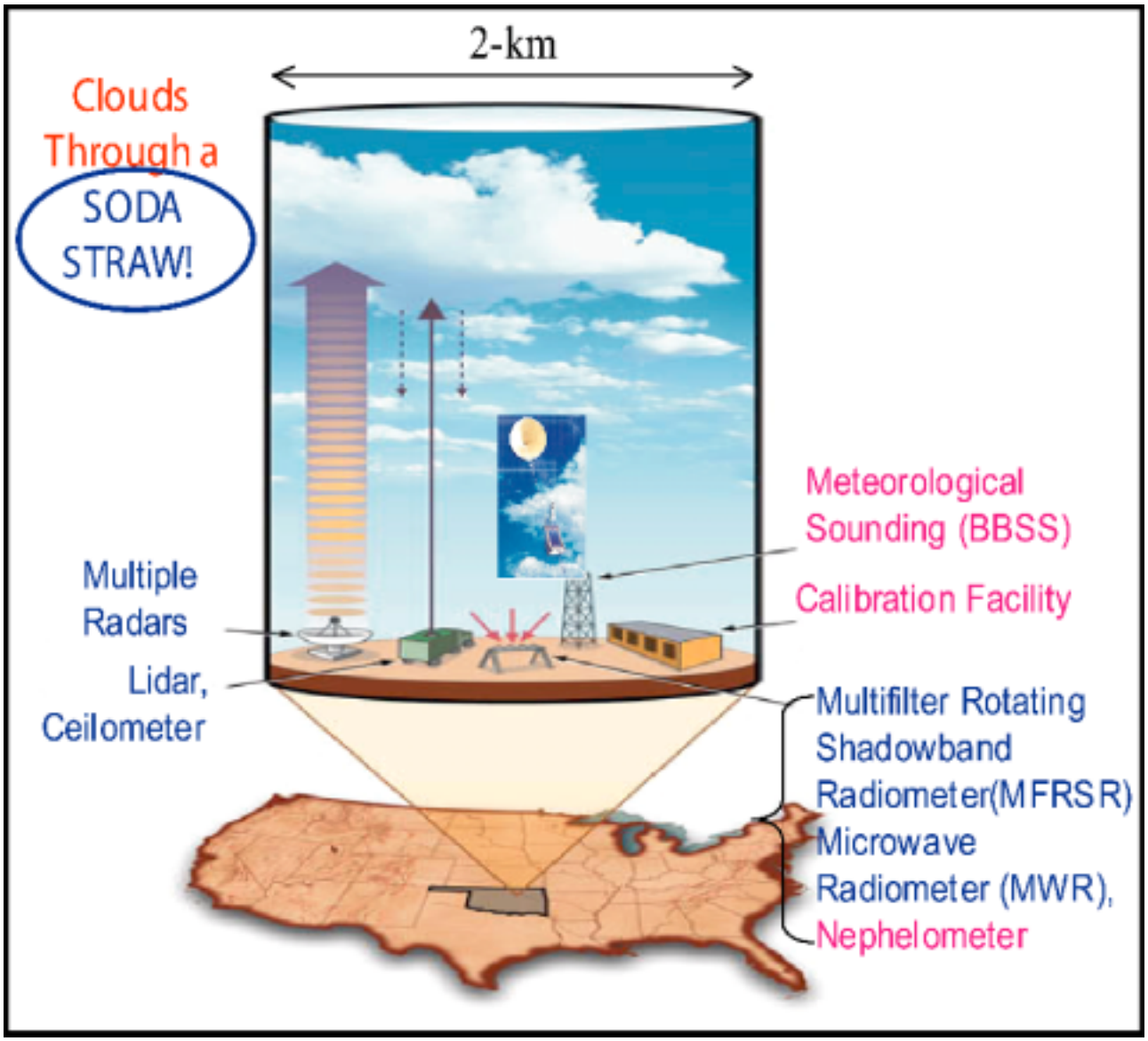

Figure 1. Schematic of ground-based remote sensing of cloud properties at the ARM SGP site in North Central Oklahoma.

Objective

Here, we use ground-based remote sensing of cloud optical depth (τ_c) and liquid water path (LWP) to determine the dependence of optical depth on LWP. One of the goals is to examine the characteristics of cloud drop effective radius (r_e) and investigate its relationship to aerosol concentration using ARM data for the year 2000.

Table 1. Summary of Primary Instrumentation

Instrument	Measured Quantities	Comments	Temporal resolution
ARSCL (Active Remotely Cloud Locations)	Cloud mask	Best estimates of MMCR, Ceilometer, Lidar	10 s
MFRSR (MultiFilter Rotating Shadowband Radiometer)	Optical depth	Mainly at 415nm Measures I_{direct} and I_{total} by blocking techniques	20 s
MWR (Microwave Radiometer)	LWP	Microwave brightness T by a dual channel of 23.8, 31.4 GHz. Accuracy ±30 g m^{-2}.	20 s
BBSS (Balloon Borne Sounding System)	T, RH, ws, wd	6 hour interval (3 hour for IOP)	10 s
Nephelometer	σ_{sp}*	< 1-μm diameter At 450, 550, 700nm	1 min

* IAP (In Situ Aerosol Profiling) measures vertical distributions of σ_{sp} & σ_{ap} 2-3 times a week.

Methodology

Most Favorable Cloud Type

- Complete overcast needed for the determination of τ_c by using multi-filter rotating shadowband radiometer (MFRSR).
- Low level liquid water clouds without overlying cloud.
- Clouds in boundary layer should be related to aerosol at the surface.

Case Selection and Data Retrieval

- Wide-spread low-level and thin cloud layer selected and not interfered by higher-level cirrus ice clouds.
- Completely overcast cloudy situations screened using shaded and unshaded irradiances measured by pyranometers, and confirmed by the estimation of clear-sky cover (Long and Ackerman 2000).

- Cloud optical depth (τ_c) obtained using the observed atmospheric transmittance, and surface albedo (Min and Harrison 1996).

- Cloud LWP measured by a microwave radiometer used to obtain r_e of cloud droplets.

Dependence of Transmittance on Cloud Optical Depth

Figure 2 shows the strong dependence on cloud optical depth evaluated with a radiative transfer model SBDART (Ricchiazzi et al. 1998) based on the discrete ordinate radiative transfer (DISTORT) algorithm for discrete-ordinate-method radiative transfer (Stamnes et al. 1988). Transmittance is sensitive to optical depth and solar zenith angle (SZA), but relatively insensitive to cloud drop r_e.

Cloud optical depth displays a nearly linear dependence of optical depth on the inverse of transmittance, again quite insensitive to the value of r_e employed in the retrieval. This insensitivity allows optical depth to be retrieved without a priori knowledge of r_e.

For the results presented here, τ_c is retrieved by a dependence of transmittance on cloud optical depth. A nonlinear least square method, implemented through the linearized iteration (Bevington 1969), in conjunction with an adjoint formulation of radiative transfer to speed up the computation (Min and Harrison 1996).

Time Series of Cloud Properties

Figure 3 indicates well defined single cloud layer below 1 km. The matching of total and diffuse irradiances from 1300 to 1840 Universal Time Coordinates (UTC) is further indication of total overcast conditions. Optical depth (τ_c) and LWP tend to track each other over the course of day, indicative of a more or less constant proportionality between them during the complete overcast day, notably, as LWP increases (decreases), τ_c increases (decreases) despite being measured by completely different instruments, despite being measured by completely different measurements with different field of view. The method of determining τ_c presumes horizontal homogeneity. Satisfaction of this requirement is indicated by the temporal homogeneity of the several traces. And, examination of LWP during the intermittent drizzle demonstrated that total LWP was not influenced by drizzle. On March 15 (Figure 4), the low-level warm cloud existed below 2 km the entire day. Optical depth and LWP exhibited similar fluctuations during the overcast period, with a roughly linear dependence of τ_c on LWP. Until 1700 UTC, cloud layer was confined to 1 km and aerosol scattering coefficient also began to decrease when mixed layer height increased from the sounding.

Relationship Between Cloud Optical Depth and LWP

Scatterplots of τ_c against LWP show the controlling influence of LWP on τ_c (Figure 5). To the extent that data can be represented as a linear dependence on a line through the origin, then the data are indicative of a single value of r_e. Optical depth exhibited a roughly linear dependence on LWP with

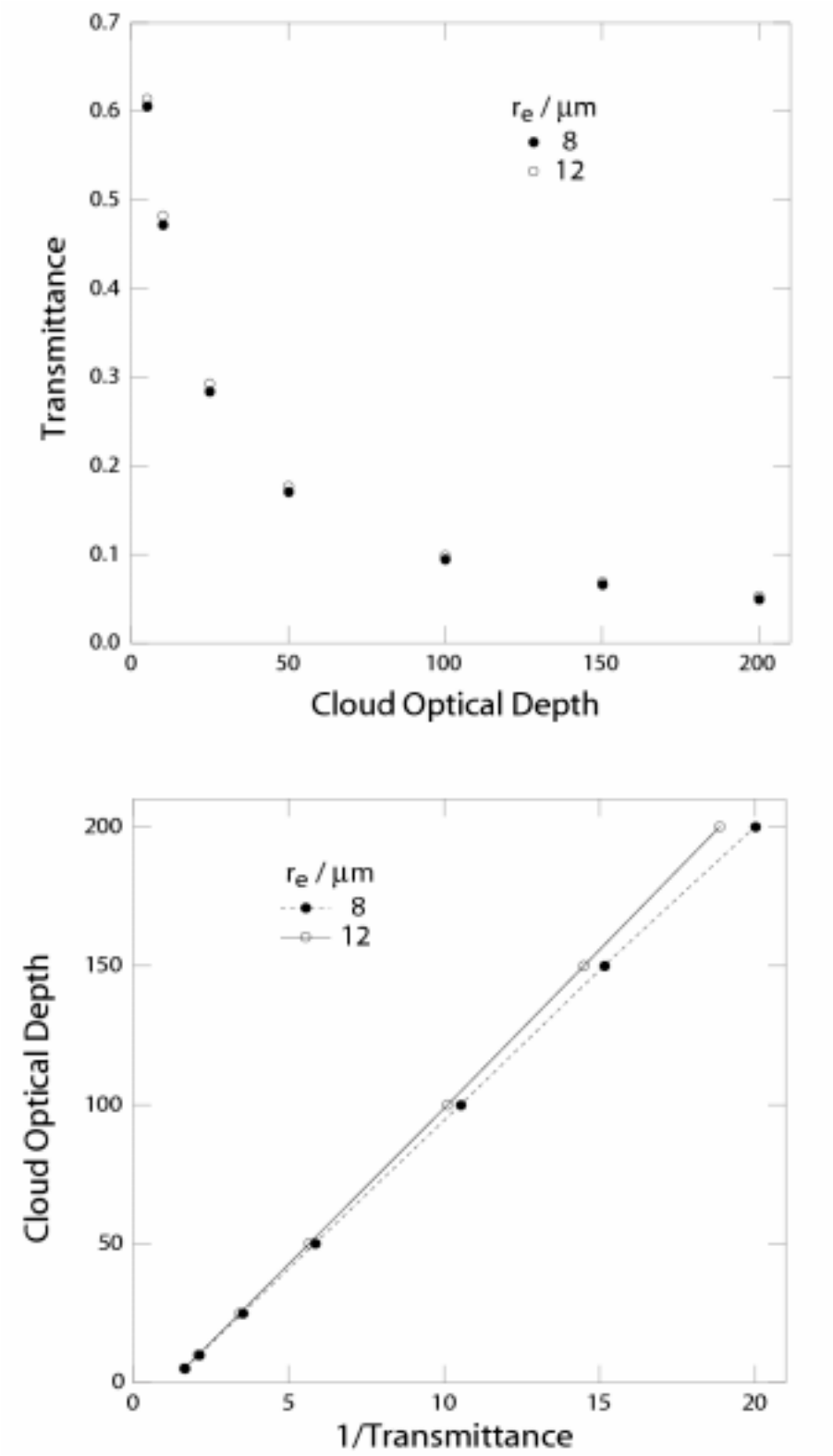

Figure 2. Calculated atmospheric transmittance as a function of optical depth, and dependence of optical depth as a function of inverse of atmospheric transmittance.

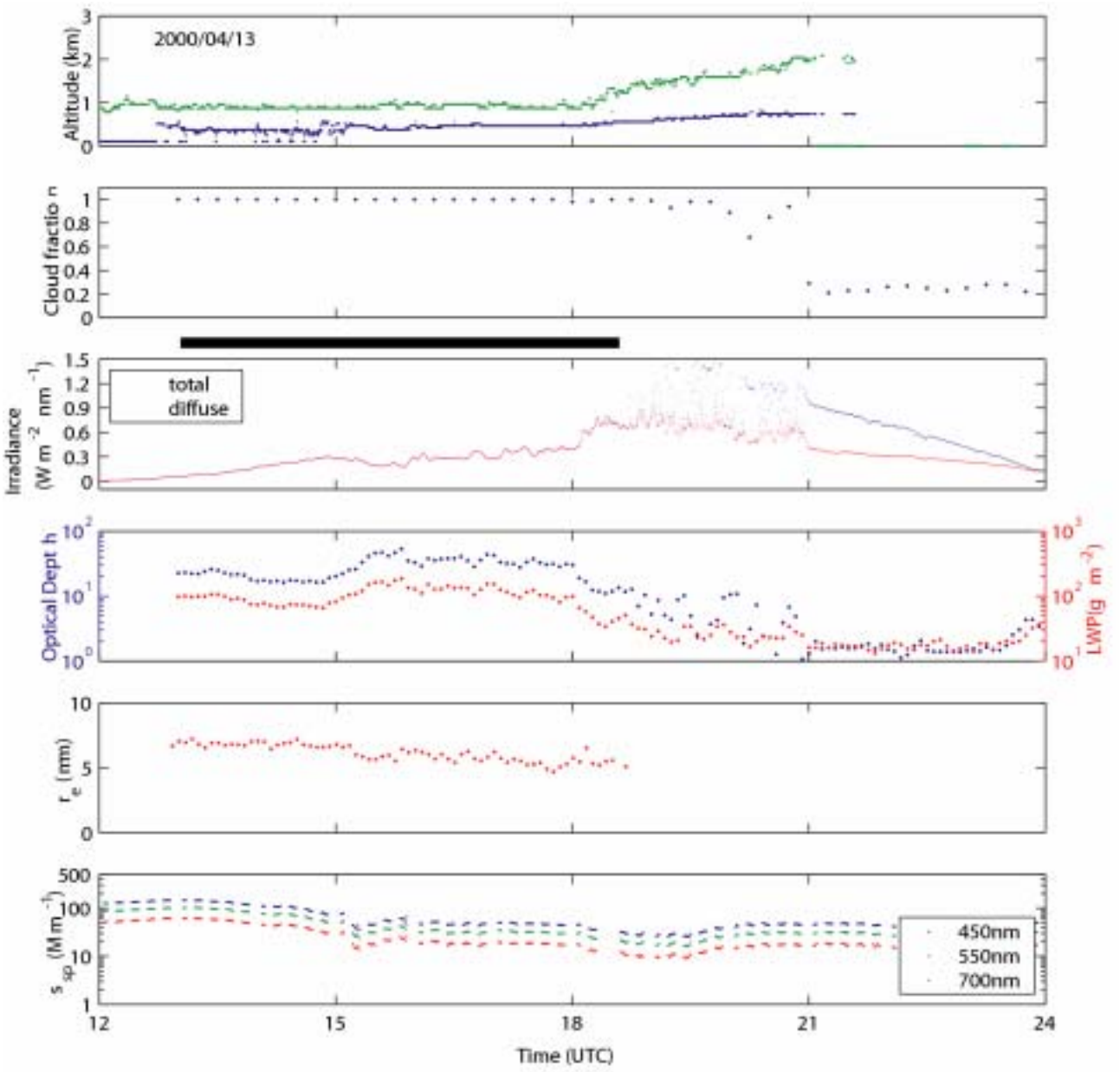

Figure 3. Time series of cloud boundaries, total horizontal and diffuse irradiances, cloud optical depth, LWP, r_e of cloud droplets and aerosol scattering coefficient on April 13. The thick black line indicates the completely overcast period.

slopes that varied day to day, especially plots of 2/18, 3/19, 4/13, and 7/23 exhibiting a nearly linear dependence of τ_c on LWP, indicating the r_e of around 5.2-5.6 μm. It suggests that the cloud should be considered to be horizontally homogeneous and consist of relatively uniform particles with the vertically integrated r_e. Overall the plots showed steeper slopes than those of marine clouds (Schwartz et al. 2002).

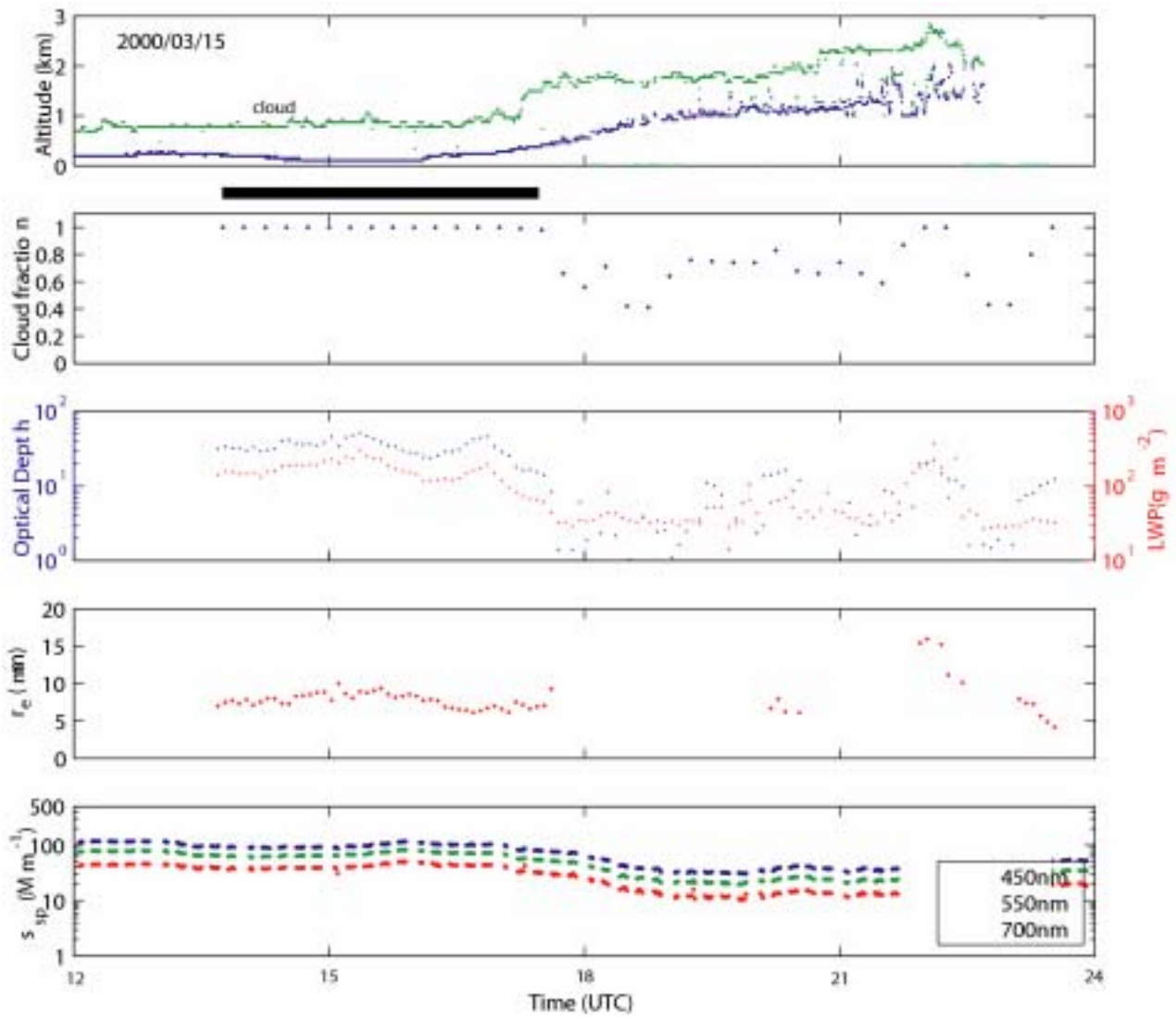

Figure 4. Time series of cloud boundaries, cloud fraction, cloud optical depth, LWP, r_e of cloud droplets and aerosol scattering coefficients on March 15.

Relationship of Effective Radius to Aerosol

Figure 6 examines the relationship of r_e to aerosol light scattering coefficient σsp on the average of each event. Effective radius was negatively albeit weakly correlated with σsp. The case of October 26 is excluded; for this case, unusually, a mixed layer did not develop even during the daytime and thus the cloud was decoupled from the surface. The slope of $\log(r_e)$ vs. $\log(\sigma_{sp})$ is -0.16 (r = 0.47). The magnitude is consistent with attribution of varying r_e to variation in the aerosol that served as nuclei for droplets comprising cloud.

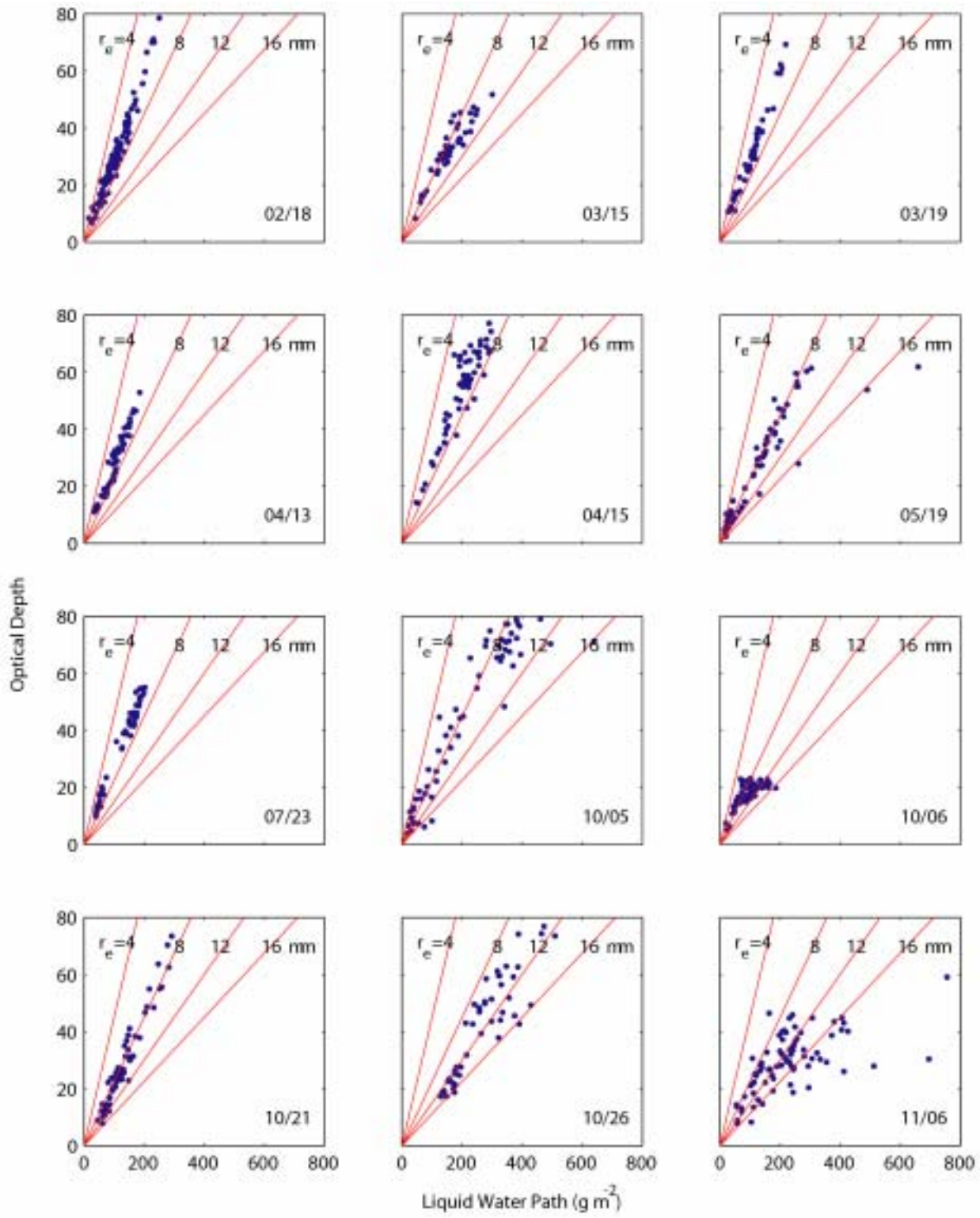

Figure 5. Scatterplots of cloud optical depth against LWP. Lines denote cloud optical depth for indicated constant values of r_e.

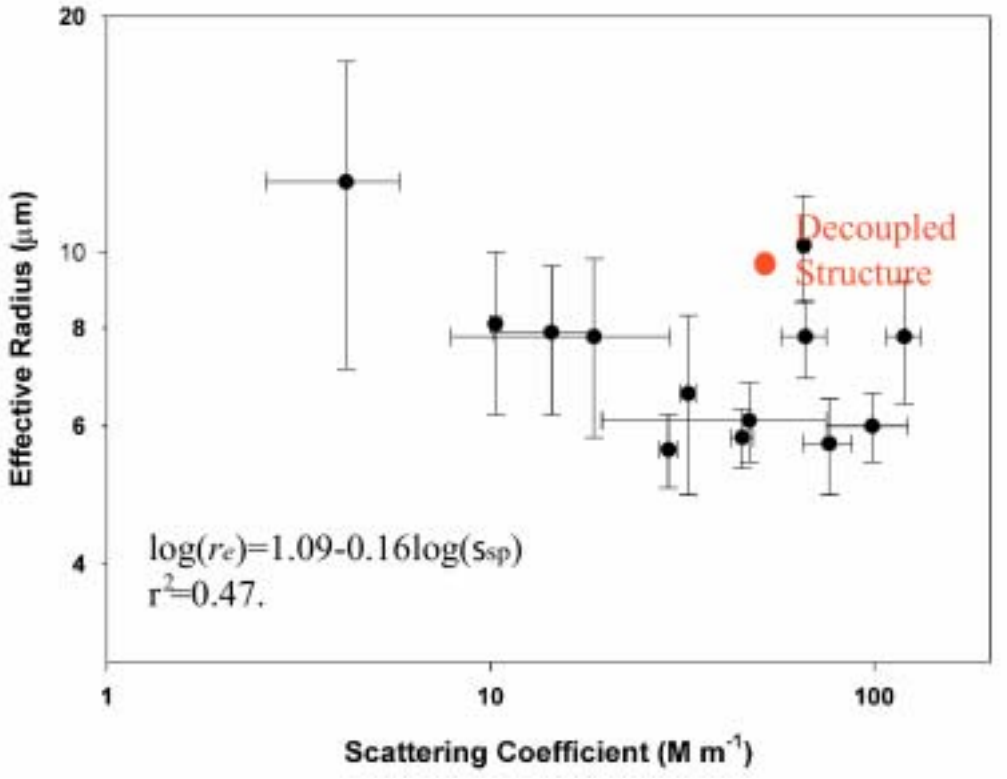

Figure 6. Scatterplots showing r_e vs. scattering coefficient based on the average of each event. Error bar indicates the standard deviation of r_e and σsp, respectively.

From the time series of cloud properties (Figures 3 and 4), there generally seemed to be no systematic correlations between r_e and σ_{sp} within a day. On April 13 (Figure 3), r_e decreased slightly from 6.8 - 7.2 μm to 5.8 - 6.5 μm especially around 1500 UTC, when σ_{sp} also decreased 66.7 to 36.0 Mm^{-1}, not consistent with the expectation of enhancement associated with greater aerosol loading and decreased r_e. This could be explained by the vertical decoupled structure of In situ Aerosol Profile (IAP, Figure 7) with discontinuity right over the mixed layer. Vertical decoupled structure was indicated around 1 km AGL together with sharp decrease of σ_{sp} from 70 - 80 to 2 - 10 Mm^{-1}. Apparently upper level cloud for this period seems to be not related to aerosol at the surface.

Discussion

Dependence of r_e on potential temperature gradient and wind shear is compared for below cloud, in cloud layer and above the mixed layer (ML). Wind shear exhibited anti-correlation with r_e only above the ML (Figure 8). Lower r_e is associated with the higher wind shear that could increase the ascent rate of air parcels in cloud, which might facilitate the cloud supersaturation, and finally decrease r_e. The systematic difference in cloud spherical albedo for a given LWP attributable to difference in r_e is evident for the several days (Figure 9). The change in shortwave radiation budget associated with changes in r_e is evaluated using SBDART model. For a LWP = 100 g m^{-2}, τ_c for r_e equal to 9.2, 6.6 and 5.2 μm are 16.3, 22.7, and 28.8. For SZA 60˚ and vegetated surface, the corresponding broadband

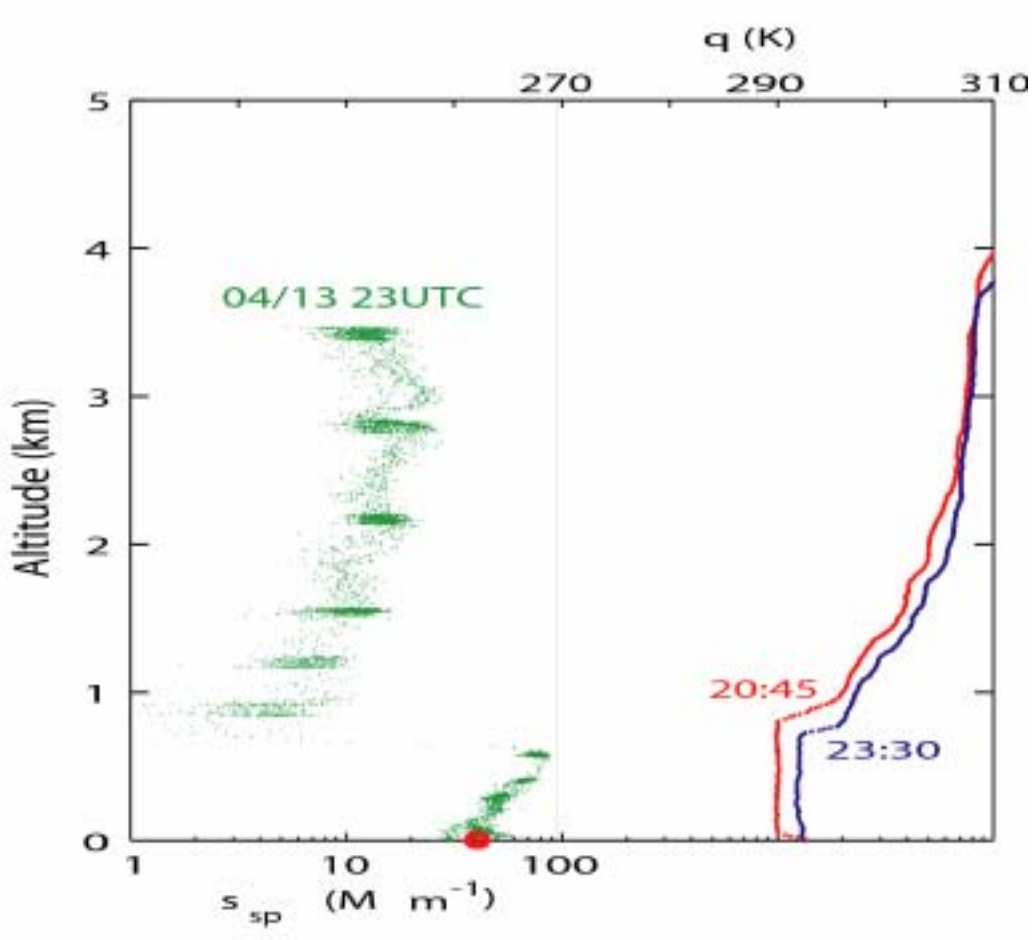

Figure 7. Vertical profiles of aerosol scattering coefficients from IAP flight and potential temperature from Balloon-Borne Sounding System on April 13.

irradiance at top of the atmosphere are 286, 256, and 236 W m^{-2}. The decrease in r_e from 9.2 to 5.2 μm and resultant increase in τ_c decrease the absorbed irradiance by 50 W m^{-2}.

Conclusions

Ground-based remote sensing of cloud optical depth and LWP has been used to determine the dependence of optical depth on LWP. The characteristics of cloud droplet r_e are investigated using SGP ARM archive for the whole year 2000.

Optical depth and LWP tend to track each other over the course of each episode, indicative of a roughly linear dependence between them during the complete overcast situation. Additionally the slope of τ_c against LWP is inversely proportional to r_e. Effective radius exhibits negative correlation with σ_{sp} at the surface, expected for the Twomey mechanism, although other factors such as vertical decoupling structure of aerosol and vertical wind shear appear to influence r_e. Notably, the decrease in r_e and the

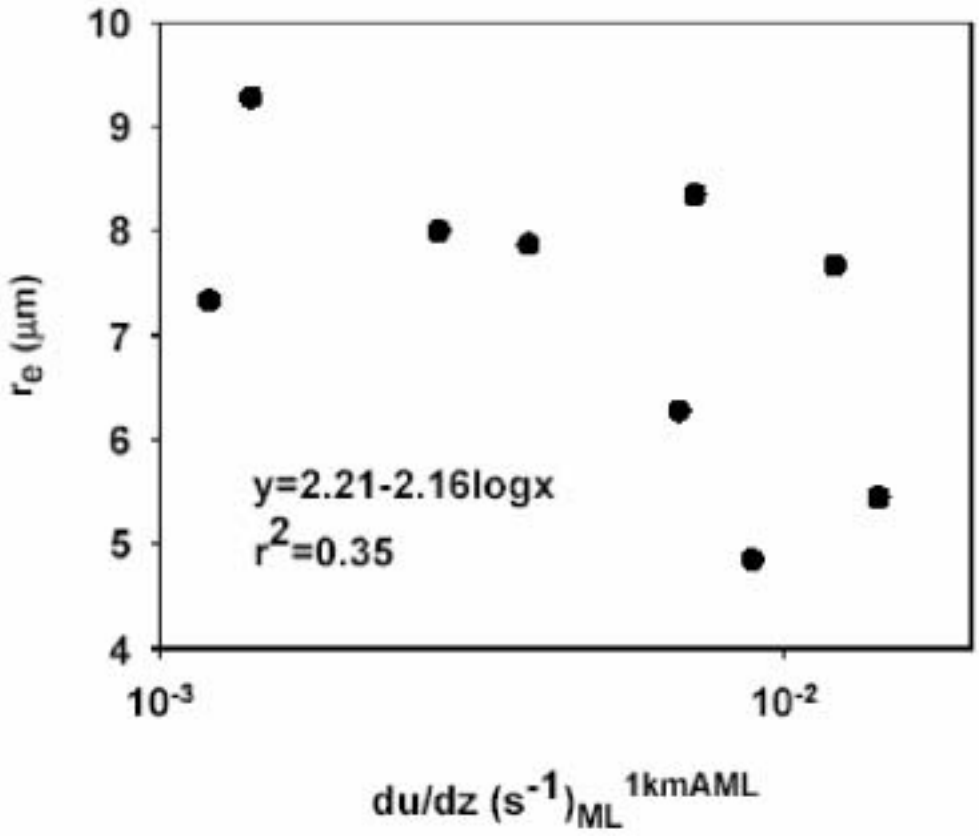

Figure 8. Relationships of r_e with wind shear from the ML top to 1 km above the ML top.

enhancement of τ_c results in the increase in cloud albedo and decrease in absorption of solar radiation. Future work would be to examine how well surface aerosol measurements could represent the overlying atmospheric column, using in situ aircraft measurement and Raman lidar. The influence of turbulent factors on r_e should be investigated in more accurately quantifying the aerosol influence on cloud microphysics.

Acknowledgments

We thank J. Ogren and P. Sheridan for 1-minute averages of σ_{sp} with IAP flight data, and C. N. Long for the information of the fractional sky cover. This work was supported in part by U.S. Department of Energy's Atmospheric Radiation Measurement Program and B.-G Kim was supported in part by the Korean Science and Engineering Foundation

Corresponding Author

Byung-Gon Kim, bgkim@bnl.gov

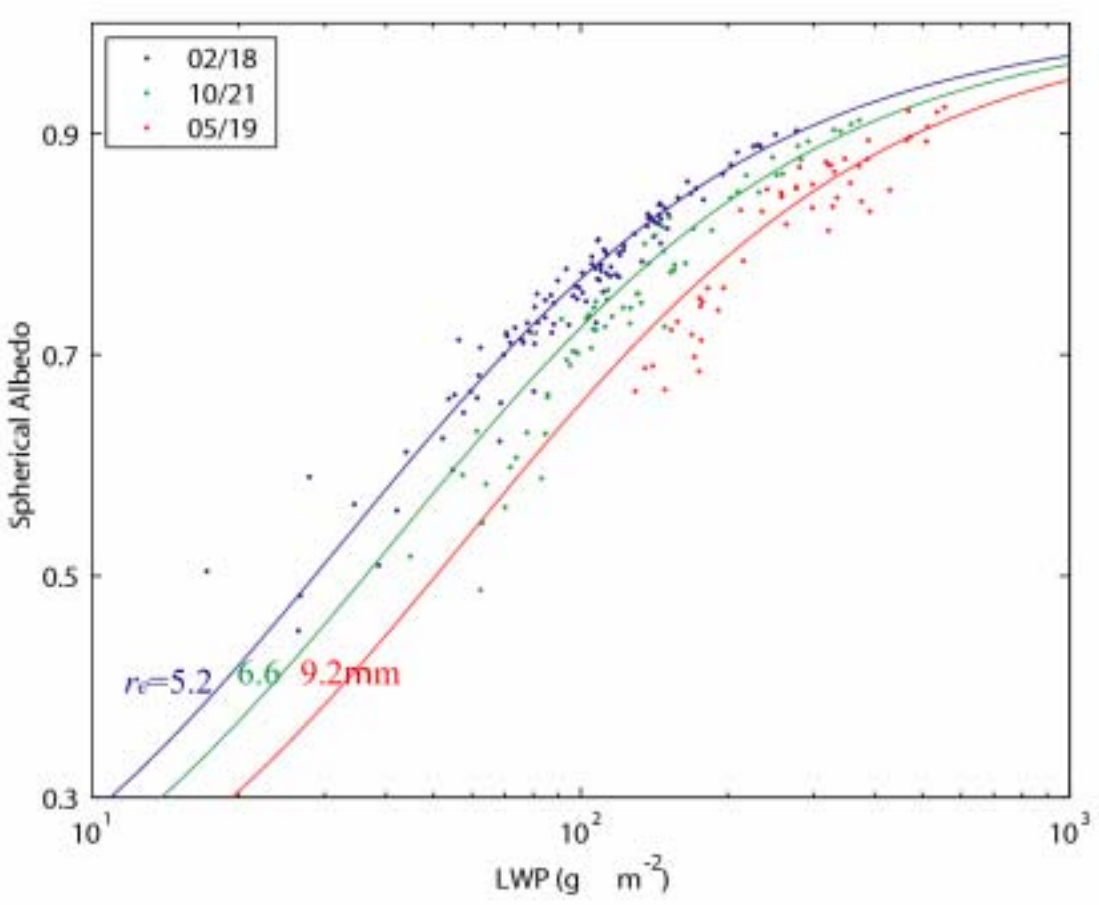

Figure 9. Cloud spherical albedo as a function of cloud LWP. Curve denotes cloud albedo for indicated constant values for r_e.

References

Albrecht B. A., C. S. Bretherton, D. Johnson, W. H. Schubert, and A. S. Frisch, 1995: The Atlantic Stratoumulus Transition Experiment—ASTEX. *Bull. Amer. Meterol. Soc*., **76**, 889-904.

Bevington, P. R., 1969: "Data reduction and error analysis for the physical sciences." *Mc-Graw-Hill*, New York.

Brenguier J. L., P. Y. Chuang; Y. Fouquart, D. W. Johnson, F. Parol, H. Pawlowska, J. Pelon, L. Schüller, F. Schröder, and J. Snider, 2000: An overview of the ACE-2 CLOUDYCOLUMN closure experiment. *Tellus*, **B 52**, 815-827.

Long, C. N., and T. P. Ackerman, 2000: Identification of clear skies from broadband pyranometer measurements and calculation of downwelling shortwave cloud effects. *J. Geophys. Res*., **105**, 15,609-15,626.

Min, Q., and L. C. Harrison, 1996: Cloud properties derived from surface MFRSR measurements and comparison with GEOS results at the ARM SGP site. *Geophys. Res. Lett*., **23**, 1641-1644.

Radke, L. F., J. A. Coakley Jr., and M. D. King, 1989: Direct and remote sensing observations of the effects of ships on clouds. *Science*, **246**, 1146-1149.

Ricchiazzi, P., S. Yang, C. Gautier, and D. Sowie, 1998: SBDART: A research and teaching software tool for plane-parallel radiative transfer in the Earth's atmosphere. *Bull. Amer. Meteorol. Soc*., **79**, 2101-2114.

Schwartz, S. E., and A. Slingo, 1996: Enhanced shortwave cloud radiative forcing due to anthropogenic aerosols. In *Clouds, Chemistry and Climate--Proceedings of NATO Advanced Research Workshop*. P. Crutzen and V. Ramanathan, Eds., pp. 191-236, Springer, Heidelberg.

Stamnes, K., S. C. Tsay, W. J. Wiscombe, and K. Jayaweera, 1988: Numerically stable algorithm for discrete-ordinate-method radiative transfer in multiple scattering and emitting layered media. *Applied Optics*, **27**, 2502.

Stokes, G. M., and S. E. Schwartz, 1994: The Atmospheric Radiation Measurement (ARM) Program: Programmatic Background and Design of the Cloud and Radiation Testbed. *Bull. Amer. Meteorol. Soc*., **75**, 1201-1221.

Twomey, S., 1977: Atmospheric Aerosols. *Elsevier*, New York.